

## Stabilization of Ion-Temperature-Gradient–Driven Tokamak Modes by Magnetic-Field Gradient Reversal

M. Fivaz,<sup>1</sup> T. M. Tran,<sup>1</sup> K. Appert,<sup>1</sup> J. Vaclavik,<sup>1</sup> and S. E. Parker<sup>2</sup>

<sup>1</sup>*Centre de Recherches en Physique des Plasmas, Association Euratom-Confédération Suisse,  
Ecole Polytechnique Fédérale de Lausanne, PPB, 1015 Lausanne, Switzerland*

<sup>2</sup>*Department of Physics, University of Colorado, Boulder, Colorado 80309*

(Received 5 December 1996)

Global gyrokinetic particle simulations have been used to search tokamak configurations which are stable against the ion-temperature-gradient–driven (ITG) modes commonly held responsible for the core anomalous ion heat transport. The stable configurations are characterized by strongly reduced or reversed  $\nabla B$  drifts on the low-field side. Since excellent transport properties have been observed in high  $\beta_p$  (poloidal beta) tokamak experiments, we conjecture, as a result of our simulations, that this may be due to the stabilization of ITG modes by the reduction of the  $\nabla B$  drifts. [S0031-9007(97)03019-6]

PACS numbers: 52.55.Fa, 52.35.Kt, 52.55.Dy, 52.65.Tt

Ion-temperature-gradient–driven (ITG) instabilities are now commonly held responsible for the turbulence giving rise to anomalous ion heat transport in the core of tokamaks; ITG-based transport models have been claimed to predict successfully the plasma thermal transport over a wide range of parameters [1–3]. The reduction of this transport would be of great help in the achievement of a fusion reactor; configurations that are free of these instabilities are of very high interest. An effort has recently been made to find such configurations; e.g., oblate plasmas [4] and plasmas with sheared rotation (e.g., [2] and [5]) have been discussed as routes to ITG-mode stabilization. We propose here another route to ITG stability: the reduction of the  $\nabla B$  drift on the low-field side of the torus.

In this Letter, we study finite-pressure effects on ITG instabilities using the first global gyrokinetic particle-in-cell codes which work with full finite-pressure MHD equilibrium data. We note that microinstabilities in general equilibria were previously studied in the ballooning limit [6]. With respect to global ITG stability, we find that the dominant effect is related to the particle  $\nabla B$  drift on the low-field side of the torus: The growth rates decrease with decreasing  $\nabla B$  drift. In fact, the configurations are stable when  $\nabla B$  is close to reversal.

The ITG instability takes its free energy from the ion temperature gradient. It can be destabilized by the parallel motion (slab ITG), the poloidal magnetic drifts due to toroidicity (toroidal ITG), and the trapped-ion precession (trapped ion mode). The latter two destabilizing mechanisms are related to the magnetic drift,

$$\vec{v}_d = \frac{v_{\parallel}^2 + \frac{1}{2}v_{\perp}^2}{\Omega B^2} \vec{B} \times \nabla B + \frac{v_{\parallel}^2}{\Omega B^3} \vec{B} \times \mu_0 \nabla p, \quad (1)$$

where  $\vec{B}$  denotes the magnetic field,  $\Omega$  the ion cyclotron frequency,  $v_{\parallel}$  and  $v_{\perp}$  the parallel and perpendicular particle velocities, and  $p$  the plasma pressure. From a wave-particle interaction diagnostic implemented in one of our codes, we find that particles with  $v_{\perp} \gg v_{\parallel}$  contribute most

to the instability. In a simple analysis which helps to understand the simulation results to be presented, the second term in Eq. (1) can therefore be neglected.

For  $k_{\parallel} = 0$  and  $k_{\psi} = 0$ , the wave vector reduces to  $\vec{k} = nq\nabla\chi - n\nabla\varphi$ ,  $\chi$  being the straight-field-line poloidal angle [7],  $\varphi$  the toroidal angle,  $n$  the toroidal mode number, and  $q$  the safety factor. In the local and fluid limits, the drift frequencies may then be defined as

$$\omega_d \equiv \vec{k} \cdot \vec{v}_d = \frac{nT_i}{e} \frac{\partial}{\partial\psi} \ln B \quad (2)$$

and

$$\omega_{Ti}^* \equiv \frac{\vec{k} \times \vec{B}}{eB^2} \cdot \nabla T_i(\psi) = \frac{nT_i}{e} \frac{d}{d\psi} \ln T_i, \quad (3)$$

where  $T_i$  is the ion temperature and  $\psi$  the poloidal magnetic flux of the equilibrium.

Focusing on the toroidal ITG regime and taking the local and fluid limits of the gyrokinetic equation in the absence of a density gradient, one obtains the dispersion relation [8,9],

$$\omega^2 + \omega_{Ti}^* \omega_d = 0, \quad (4)$$

i.e., the mode is locally stable for  $\omega_d > 0$  (favorable gradient region) and locally unstable for  $\omega_d < 0$  (unfavorable gradient region), the growth rate increasing with  $|\omega_d|$ . Similar arguments can be made for trapped-particle-driven modes.

A direct way of stabilizing the mode is to lower the magnetic drift on the low-field side of the torus, thereby reducing  $\omega_d$ . In configurations where the magnetic field has a minimum, the  $\nabla B$  drift is even reversed and the unfavorable gradient region is turned into a favorable gradient region. Figure 1 shows the contours of  $\omega_d$  in two configurations: (a) the usual case of a low  $\beta_p$  equilibrium and (b) of a higher  $\beta_p$  equilibrium where the drifts are reversed over most of the plasma. The dashed region corresponds to negative values, i.e., the unfavorable gradient region. Configuration (a) has a wide region of

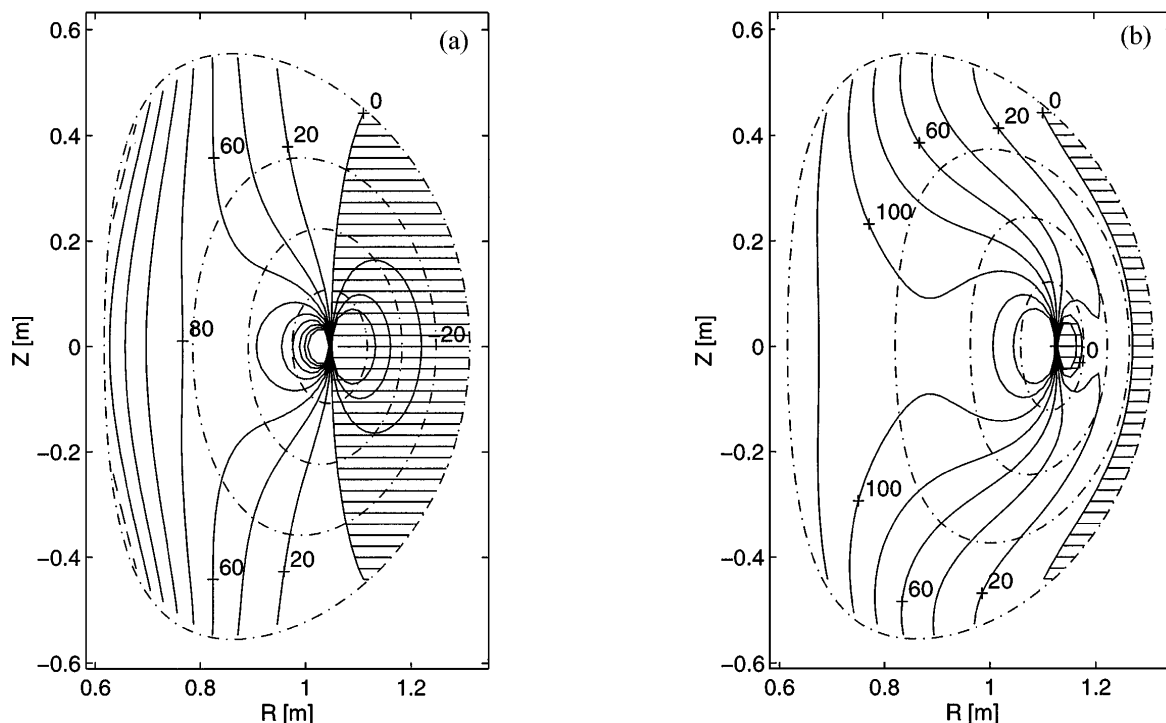


FIG. 1. Contours of the drift frequency  $\omega_d$  (arbitrary units); the hatched zones correspond to negative values, i.e., to the unfavorable gradient region. The dashed lines correspond to the magnetic surfaces  $s = 0.25$ ,  $s = s_0 = 0.5$ ,  $s = 0.75$ , and  $s = 1.0$ . (a) Standard configuration with  $\beta = 3\%$  and local  $\beta_p(s = s_0) = 1.2$ . This configuration is unstable for ITG modes. (b) Configuration with drift reversal on the low-field side,  $\beta = 4.4\%$ , local  $\beta_p(s = s_0) = 4.9$ . This configuration is stable for all toroidal mode numbers.

unfavorable gradient and is expected to be unstable to global ITG modes. The configuration (b) has favorable gradients over most of the plasma and is expected to be stable to global modes.

In our simulations, the plasma is modeled with gyrokinetic ions [10] and adiabatic electrons. An axisymmetric equilibrium magnetic structure (solution of the Grad-Shafranov equation [11]) is provided by the MHD equilibrium code CHEASE [12]. The full plasma cross section is considered in the simulations. We follow the time evolution of electrostatic, quasineutral perturbations of a local Maxwellian equilibrium distribution function, using two different particle-in-cell (PIC) codes running on a massively parallel CRAY-T3D. The first is a linear finite element PIC code [13] solving for the electrostatic potential in nonorthogonal magnetic coordinates while the second is a new version of the nonlinear code ORB [14] that has been modified [15] to accept the same MHD equilibrium data as the finite element code. Here it is used in its linear version only. Both codes give essentially the same results. The finite element code shows good convergence to a unique solution when we enhance the numerical resolution, for example, by increasing the number of particles [16], increasing the number of grid points, or decreasing the time step, even in the absence of a filtering scheme. Comparisons with eigenvalue codes, both radially global [17] and in the ballooning limit, show good agreement. In the cases studied here, a converged solution is ob-

tained with  $\sim 10^6$  particles,  $\sim 500$  grid points, and  $\sim 500$  time steps.

Other effects have been studied by many authors, e.g., electromagnetic perturbations [6,18] and/or trapped electrons [19,20]. Although their influence on our results will have to be investigated in future work, there are reasons to believe that the general conclusions will not be changed; we note, for instance, that the drives related to trapped electrons and to the ion physics are both determined by the radial gradient of the magnetic field.

A set of JET-shaped equilibria was produced, varying the sources (current and pressure profiles) in the Grad-Shafranov equation. The boundary shape and the value of the safety factor  $q = 2$  at a given radial point,  $s = s_0 = 0.5$ , have been kept constant. Here,  $s$  is the square root of the normalized poloidal flux,  $s = (\psi/\psi_0)^{0.5}$ , and acts as the radial variable. Other parameters are the major radius  $R_0 = 0.96$  m, minor radius  $a = 0.35$  m, elongation  $E = 1.6$ , triangularity  $\delta = 0.3$ , and  $B_0 = 1$  T. The set covers a wide range of parameters:  $0 < \beta < 4.5\%$ ,  $0 < \beta_p < 2.5$ , shear  $0.3 < \hat{s} < 0.9$  at  $s = s_0$ , internal inductance  $0.5 < l_i < 1$ , and Shafranov shift  $0 < c < 0.5a$ .

We then studied the stability of ITG modes in these equilibria, using a flat density profile, typical of the core of an H mode, and flat electron temperature  $T_e = 1$  keV. The ion temperature profile was such that the logarithmic ion temperature gradient peaks at  $s = s_0$ , effectively confining the most unstable mode around  $s = s_0$ :

$$\frac{1}{T_i} \frac{dT_i}{ds} = -\kappa \cosh^{-2} \left( \frac{s - s_0}{\Delta s} \right), \quad (5)$$

where  $\kappa = 1/0.35$ ,  $\Delta s = 0.42$ , and  $T_i(s = s_0) = 1$  keV. As a consequence of these parameters, one obtains  $a/\rho_i = 76$  where  $\rho_i$  is the deuterium Larmor radius and  $L_T/R_0 = 0.127$ , where  $L_T$  is the temperature gradient scale length. The simulation provides the most unstable mode for a given toroidal mode number  $n$ .

The simulations confirm the simple analysis following Eqs. (2)–(4). The configuration (a) is unstable for several toroidal mode numbers  $n$ ; the corresponding growth rates are shown in Fig. 2. The mode amplitudes peak in the negative  $\omega_d$  region of unfavorable gradient. They are destabilized mainly by the poloidal magnetic drifts, but also somewhat by the parallel motion and the trapped ion precession, and thus can be classified as toroidal ITG modes with small slab ITG and trapped-ion character.

The configuration (b) is found to be fully stable, i.e., stable for all values of  $n$ , despite the flat density ( $\eta_i = \infty$ ) and the value of  $L_T/R_0 = 0.127$ , which usually lead to high growth rates [21]. This is because  $\nabla B$  is favorable everywhere around  $s = s_0$ , where the ion temperature gradient is large. Note that a much stronger temperature gradient can give the mode a strong slab ITG character and therefore destabilize it despite the favorable magnetic field gradient.

For further analysis of these results, we restrict ourselves to the surface  $s = s_0$ , and define the drift frequency ratio  $\epsilon = -\omega_d/\omega_{Ti}^*$ , its local value on the low-field side of the mid-plane  $\epsilon_l$  and its magnetic surface average,

$$\langle \epsilon \rangle = -\frac{1}{\oint dl/B} \oint \frac{\omega_d}{\omega_{Ti}^*} \frac{dl}{B}. \quad (6)$$

We note that  $\omega_{Ti}^*$  is a magnetic surface quantity and commutes with the surface average in  $\langle \epsilon \rangle$ . In configurations similar to configuration (a), the positive (favorable gradient) and negative (unfavorable gradient) contributions from  $\omega_d$  almost cancel, and  $\langle \epsilon \rangle \approx 0$ . In drift-reversed equilibria such as configuration (b), the average has only

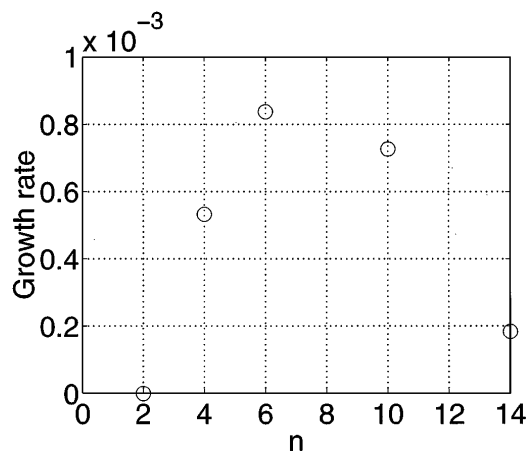


FIG. 2. Growth rate (normalized to the ion cyclotron frequency) as a function of toroidal mode number for the configuration shown in Fig. 1(a).

positive contributions and  $\langle \epsilon \rangle$  is larger. Figure 3 shows the growth rate of the  $n = 6$  mode versus  $\langle \epsilon \rangle$  for all the configurations studied. Above  $\langle \epsilon \rangle = 0.02$ , the growth rate decreases linearly with  $\langle \epsilon \rangle$  up to full stability. The points with  $\langle \epsilon \rangle < 0.02$  correspond to equilibria where the drifts are so strong ( $|\epsilon_l| \geq 0.1$ ) that increasing them further becomes stabilizing. Similar results are obtained for usual model configurations [21]; in such a case,  $|\epsilon_l| = L_T/R_0$ ,  $\langle \epsilon \rangle \approx 0$ , and the ITG growth rate decreases for  $|\epsilon_l| \geq 0.1$ .

We found that  $\langle \epsilon \rangle$  is, in fact, the best indicator for ITG stability, but two other quantities come near. The first is the traditional MHD magnetic well [22], which is also a measure for the surface average of  $\nabla B$  and shows excellent correlation with the growth rate [13]. Similar conclusions were drawn in [23] for purely trapped particle modes. The second is the local (at  $s = s_0$ ) value of  $\beta_p$  which is related to  $\nabla B$  drift reduction through the gradient of the toroidal magnetic field. In contrast, the growth rates do not correlate well with the global value of  $\beta_p$  or with parameters such as the shear at  $s = s_0$ , the Shafranov shift, the internal inductance  $l_i$ , or the normalized plasma pressure  $\beta$ . At fixed finite beta and fixed safety factor, the plasma shape can influence the reversal condition; in fact, plasma oblateness seems to increase the magnetic drift reversal [4].

There are a number of experimental discharges in various devices where the stabilization of microinstabilities by the reduction of  $\nabla B$  may have contributed to a reduction of anomalous transport. As the  $\nabla B$  drift reduction tends to occur in equilibria with high local (i.e., local to a magnetic surface) values of  $\beta_p$  [11], these equilibria should have relatively high global  $\beta_p$  as well. In several tokamaks, some high  $\beta_p$  discharges, when free of edge localized modes (ELMs), have indeed shown very good confinement properties. On JET [24] and DIII-D [25], confinement substantially better than the JET/DIII-D H-mode scaling has been obtained. On PBX-M [26], the heat diffusivity was seen to decrease in time while  $\beta_p$

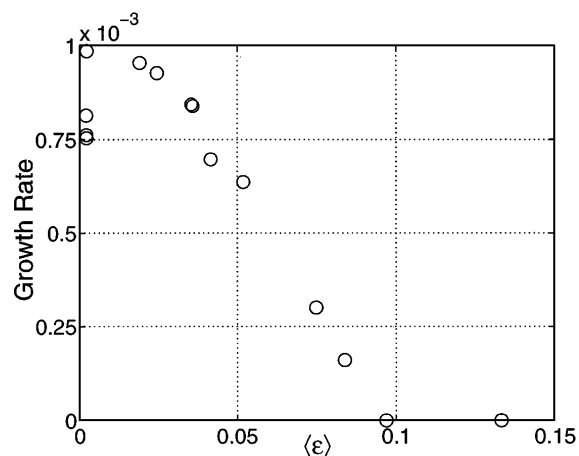


FIG. 3. Growth rate (normalized to the ion cyclotron frequency) of the  $n = 6$  mode for different configurations, as a function of the surface-averaged drift frequency ratio  $\langle \epsilon \rangle = \langle -\omega_d/\omega_{Ti}^* \rangle$  at  $s = s_0$ .

increased. On JT-60U [27–29], high  $\beta_p$  discharges showed a highly enhanced confinement leading to record-breaking neutron yields; the ion heat transport was found to be low everywhere in the core, unlike the situation when a  $H$ -mode transport barrier is present. This is consistent with a stabilization of microinstabilities by the reduction of  $\nabla B$  over a wide radial extension.

A preliminary analysis of JET equilibria with low current and relatively high  $\beta_p$  ( $\approx 1.5$ ) has shown that a reduction of  $\nabla B$  by a factor of four (compared to a usual low-beta configuration with  $B \sim 1/R$ ) can experimentally be realized. In such conditions, a drastic reduction of ITG-induced transport is expected. Detailed studies of the transport properties of such discharges should be undertaken concentrating on cases without gross MHD activity (ELMs and sawteeth).

A condition for drift reversal can be derived by noting that the unfavorable gradient occurs in the region where  $\frac{\partial B}{\partial \psi} < 0$ . Using the equation of MHD equilibrium  $\mu_0 \nabla p = (\nabla \times \vec{B}) \times \vec{B}$ , one can easily show that drift reversal occurs when

$$-\mu_0 \frac{dp}{d\psi} > \frac{1}{R} \frac{\partial R}{\partial \psi} B^2, \quad (7)$$

i.e., the pressure gradient must be sufficiently large. Since large pressure gradients can destabilize MHD modes, configurations of practical interest might have to compromise between microstability and MHD stability. In fact, the ITG stable configurations presented here are unstable to MHD ballooning modes over parts of the plasma. We note that, though not attempted here, the simultaneous optimization of ITG and MHD ballooning stability should be possible, e.g., by varying the magnetic shear.

In conclusion, we have presented global gyrokinetic PIC simulations which show that ITG modes can be stabilized by a reduction of the equilibrium  $\nabla B$  drifts. For fixed plasma shape, safety factor at half radius and ion temperature gradient, ITG stability is determined by these drifts. We expect similar tendencies for other magnetic-drift small-driven microinstabilities such as collisionless trapped particle modes. We find that, for relatively strong gradients ( $L_T/R_0 = 0.127$ ), a configuration is fully ITG stable when the  $\nabla B$  drifts are close to reversal. Such magnetic configurations do exist in some experimental discharges and should, according to our simulations, be characterized by a low level of ITG transport. We also conjecture that the experimentally observed low level in ELM-free high- $\beta_p$  discharges may be due or partly due to reduced  $\nabla B$  drifts on the low-field side.

In the near future, a serious effort should be made in analyzing experimental data from MHD-quiescent discharges, trying to correlate  $\nabla B$  reduction with ion thermal transport. On the theory side, the future search for stable configurations should not be limited to microstability but must include MHD considerations as well.

This research was supported in part by both the Cray/EPFL Parallel Application Technology Program and

the Swiss National Science Foundation. All computations have been performed on the Cray-T3D of the Ecole Polytechnique Fédérale in Lausanne. We acknowledge useful discussions with S. Brunner, F. Hofmann, L. Villard, and H. Weisen from CRPP, as well as help with JET data analysis from B. Balet, W. Heidbrink, and G. Huysmans.

- 
- [1] M. Kotschenreuther, W. Dorland, M. A. Beer, and G. W. Hammett, *Phys. Plasmas* **2**, 2381 (1995).
  - [2] R. E. Waltz, G. M. Steabler, G. W. Hammett, and J. Koenigs, Proceedings of the 16th IAEA Fusion Energy Conference, Montreal, 1996, Poster F1-CN-64/DP-7 (to be published).
  - [3] G. Bateman *et al.*, (Ref. [2]) Poster F1-CN-64/DP-7.
  - [4] M. Kotschenreuther and W. Dorland (private communication).
  - [5] M. Artun, W. M. Tang, and G. Rewoldt, *Phys. Plasmas* **2**, 3384 (1995).
  - [6] G. Rewoldt, W. M. Tang, and M. S. Chance, *Phys. Fluids* **25**, 480 (1982).
  - [7] W. D. D'haeseleer, W. N. G. Hitchon, J. D. Callen, and J. L. Shohet, *Flux Coordinates and Magnetic Field Structure* (Springer-Verlag, New York, 1991).
  - [8] X. Garbet *et al.*, *Phys. Fluids B* **4**, 136 (1992).
  - [9] F. Romanelli, *Phys. Fluids B* **1**, 1018 (1989).
  - [10] T. S. Hahm, *Phys. Fluids* **31**, 2670 (1988).
  - [11] J. Wesson, *Tokamaks* (Clarendon Press, Oxford, 1987).
  - [12] H. Lütjens, A. Bondeson, and O. Sauter, *Comput. Phys. Commun.* **97**, 219 (1996).
  - [13] M. Fivaz *et al.*, *Theory of Fusion Plasmas, International Workshop, Varenna, August, 1996* (Editrice Compositori, Società Italiana di Fisica, Bologna, 1997), p. 485.
  - [14] S. E. Parker, W. W. Lee, and R. A. Santoro, *Phys. Rev. Lett.* **71**, 2042 (1993).
  - [15] T. M. Tran *et al.*, International Sherwood Fusion Theory Conference, Philadelphia, March, 1996, Book of Abstracts 2C21 (to be published).
  - [16] M. Fivaz, K. Appert, and J. Vaclavik, *Europhysics Conference Abstracts Vol. 19C, Part IV* (European Physical Society, Geneva, 1995), p. 233.
  - [17] S. Brunner *et al.*, in Ref. [13], p. 101.
  - [18] M. Kotschenreuther, G. Rewoldt, and W. M. Tang, *Comput. Phys. Commun.* **88**, 128 (1995).
  - [19] M. Beer, Ph.D. thesis, Princeton University, 1996 (unpublished).
  - [20] R. D. Sydora, V. K. Decyk, and J. M. Dawson, *Plasma Phys. Control. Fusion* (to be published).
  - [21] J. Q. Dong, W. Horton, and J. Y. Kim, *Phys. Fluids B* **4**, 1867 (1992).
  - [22] J. P. Freidberg, *Ideal Magnetohydrodynamics* (Plenum, New York, 1987), Chap. 6.
  - [23] M. Rosenbluth and M. L. Sloan, *Phys. Fluids* **14**, 1725 (1971).
  - [24] C. D. Challis *et al.*, *Nucl. Fusion* **33**, 1097 (1993).
  - [25] P. A. Politzer *et al.*, *Phys. Plasmas* **1**, 1545 (1994).
  - [26] B. LeBlanc *et al.*, *Nucl. Fusion* **33**, 1645 (1993).
  - [27] T. Nishitani *et al.*, *Nucl. Fusion* **34**, 1069 (1994).
  - [28] M. Mori *et al.*, *Nucl. Fusion* **34**, 1045 (1994).
  - [29] Y. Kamada *et al.*, *Nucl. Fusion* **34**, 1605 (1994).